Appendix A
Neural Controller Stability Analysis

Now, the stability analysis is required for the closed loop system in (2.5) controlled by the discrete-time N-SM or N-SML controllers. In order to analyze the proposed control algorithms stability, the separation principle in discrete-time is used [54], which divides the analysis in two parts [36].

1. Minimization of the identification error.
   It can be achieved by on-line identification using EKF based algorithm as proved in Theorem 4.1 in [36]. As results of this theorem, the proposed RHONN model in (2.31) used to identify the class of system under study given in (2.5) ensures that the identification errors are semi globally uniformly ultimately bounded; moreover the RHONN weights remained bounded [36].
2. The tracking error convergence to a small bound region. It is achieved by the proposed neural controllers as will be demonstrated in the following analysis.

A.1 N-SM Controller

Due to identification error boundedness, there exists a bounded vector valued function $\Delta_{i,k}$, which is smaller; then [76]

$$x_k = \chi_k + \Delta_{i,k} \qquad i = 1, \ldots, r \tag{A.1}$$

with $\left\| \Delta_{i,k} \right\| \leq \gamma_i$, $\gamma_i > 0$ and r the number of the state. The sliding surface at $k+1$ is defined using x_k as follows

$$s_{k+1} = x_{k+1} - x_{ref,k+1} \tag{A.2}$$

E. N. Sánchez and L. Djilali, *Neural Control of Renewable Electrical Power Systems*, Studies in Systems, Decision and Control 278,
https://doi.org/10.1007/978-3-030-47443-0

Using (4.1), the sliding surface in (A.2) is calculated as

$$s(x_k, k+1) = \hat{f}(x_k, k) + B(x_k)u(x_k, k) + \Delta(x_k, k) - x_{ref,k+1} \tag{A.3}$$

and the equivalent control is determined as

$$u_{eq}(x_k, k) = -B(x_k)^{-1}\left[\hat{f}x_k, k + \Delta(x_k, k) - x_{ref,k+1}\right] \tag{A.4}$$

The discrete-time sliding mode controller proposed in (2.14) includes two cases:

- When $\left|\left|u_{eqn}(x_k, k)\right|\right| \leq u_0$

The applied control law in this case is $u_n(x_k, k) = u_{eqn}(x_{,}k, k) + u_{sn}(x_{,}k, k)$ then, by substituting $u_n(x_{,}k, k)$ in (A.3), the sliding surface is rewritten as

$$s(x_k, k+1) = k_c s(x_k, k) + \Delta(x_k, k) \tag{A.5}$$

Let define the Lyapunov function candidate $V(x_k, k) = s(x_k, k)^T s(x_k, k)$, then

$$\begin{aligned}
\Delta V(x_k, k) &= s(x_k, k+1)^T s(x_k, k+1) - s(x_k, k)^T s(x_k, k) \\
&= (k_c s(x_k, k) + \Delta(x_k, k))^T (k_c s(x_k, k) + \Delta(x_k, k)) - s(x_k, k)^T s(x_k, k) \\
&\leq (\|k_c\| \|s(x_k, k)\| + \|\Delta(x_k, k)\|)^2 - \|s(x_k, k)\|^2 \\
&\leq (\|k_c\| \|s(x_k, k)\| + \gamma)^2 - \|s(x_k, k)\|^2 \\
&\leq \|k_c\|^2 \|s(x_k, k)\|^2 + 2\|k_c\| \|s(x_k, k)\| \gamma + \gamma^2 - \|s(x_k, k)\|^2 \\
&\leq -(1 - \|k_c\|^2) \|s(x_k, k)\|^2 + 2\|k_c\| \|s(x_k, k)\| \gamma + \gamma^2 \\
&\leq -(1-\theta_1)\eta_1 \|s(x_k, k)\|^2 - \theta_1\eta_1 \|s(x_k, k)\|^2 + 2\|k_c\| \|s(x_k, k)\| \gamma + \gamma^2 \\
&\leq -(1-\theta_1)\eta_1 \|s(x_k, k)\|^2 + \gamma^2 + (-\theta_1\eta_1 \|s(x_k, k)\| + 2\|k_c\| \gamma) \|s(x_k, k)\|
\end{aligned}$$

with $\theta_1 < 1$, $\eta_1 = (1 - \|k_c\|^2)$, $\|k_c\| < 1$, and in the region $\|s(x_k, k)\| \geq \frac{2\gamma\|k_c\|}{\theta_1\eta_1}$, we obtain

$$\begin{aligned}
\Delta V(x_k, k) &\leq -(1-\theta_1)\eta_1 \|s(x_k, k)\|^2 + \gamma^2 \\
\Delta V(x_k, k) &\leq -(1-\theta_2)\eta_2 \|s(x_k, k)\|^2 - \theta_2\eta_2 \|s(x_k, k)\|^2 + \gamma^2 \\
\Delta V(x_k, k) &\leq -(1-\theta_2)\eta_2 \|s(x_k, k)\|^2
\end{aligned}$$

with $\theta_2 < 1$, $\eta_2 = (1-\theta_1)\eta_1$.

So, for the region $\|s(x_k, k)\| \geq \frac{\gamma}{\sqrt{\theta_2\beta_1}}$, yielding $\Delta V(x_k, k) \leq 0$ and the solution of system (A.5) is ultimately bounded.

- When $\left|\left|u_{eqn}(x_k, k)\right|\right| > u_0$

The following control law is applied $u_n(x_k, k) = u_0 \frac{u_{eqn}(x_k, k)}{\left|\left|u_{eqn}(x_k, k)\right|\right|}$. By substituting this control law in (A.3), the sliding surface is rewritten as

$$\begin{aligned} u_{eq}(x_k,k) &= B(x_k)^{-1}\left[s(x_k,k) - x_{ref,k} + x_k + \hat{f}(x_k,k)\right] \\ &= B(x_k)^{-1}\left[s(x_k,k) + \hat{f}_s(x_k,k)\right] \end{aligned} \tag{A.6}$$

with $\hat{f}_s(x_k,k) = -s(x_k,k) + \hat{f}(x_k,k)$, and the sliding surface is calculated as

$$\begin{aligned} s(x_k,k+1) &= \left[s(x_k,k) - x_{ref,k} + x_k + \hat{f}(x_k,k) + B(x_k)u_c(x_k,k) + \Delta(x_k,k)\right] \\ &= \left[s(x_k,k) + \hat{f}_s(x_k,k)B(x_k)u_c(x_k,k) + \Delta(x_k,k)\right] \end{aligned} \tag{A.7}$$

Let define the Lyapunov function candidate $V(x_k,k) = s(x_k,k)^T s(x_k,k)$, then

$$\begin{aligned} \Delta V(x_k,k) &= s(x_k,k+1)^T s(x_k,k+1) - s(x_k,k)^T s(x_k,k) \\ &= \left[s(x_k,k) + \hat{f}_s(x_k,k)B(x_k)u_c(x_k,k) + \Delta(x_k,k)\right] \\ &\quad \left[s(x_k,k) + \hat{f}_s(x_k,k)B(x_k)u_c(x_k,k) + \Delta(x_k,k)\right]^T \\ &\quad - s(x_k,k)^T s(x_k,k) \\ &= \left[\left(s(x_k,k) + \hat{f}_s(x_k,k)\right)\left(1 - u_0\frac{u_{eq}(x_k,k)}{\|u_{eq}(x_k,k)\|}\right) + \Delta(x_k,k)\right] \\ &\quad \left[\left(s(x_k,k) + \hat{f}_s(x_k,k)\right)\left(1 - u_0\frac{u_{eq}(x_k,k)}{\|u_{eq}(x_k,k)\|}\right) + \Delta(x_k,k)\right]^T \\ &\quad - s(x_k,k)^T s(x_k,k) \\ &\leq \left[\left\|s(x_k,k) + \hat{f}_s(x_k,k)\right\|\left(1 - \frac{\|u_0\|}{\|u_{eq}(x_k,k)\|}\right) + \|\Delta(x_k,k)\|\right]^2 - \|s(x_k,k)\|^2 \\ &\leq \left[\left\|s(x_k,k) + \hat{f}_s(x_k,k)\right\| - \frac{\|u_0\|}{\|B(x_k)^{-1}\|} + \|\Delta(x_k,k)\|\right]^2 - \|s(x_k,k)\|^2 \end{aligned}$$

Suppose that the control law $\|u_n(x_k)\| \leq u_0$ may vary within the domain [77], $\left\|\hat{f}_s(x_k,k) + \Delta(x_k,k)\right\| \leq u_0$, and $\sigma < u_0$ with $\sigma = \left\|f_{n,k} + \Delta(x_k,k)\right\|$, then

$$\Delta V(x_k,k) \leq \left[\|s(x_k,k) + \sigma\| - \frac{\|u_0\|}{\left\|B(x_k)^{-1}\right\|}\right]^2 - \|s(x_k,k)\|^2$$

$$\Delta V(x_k,k) \leq 2\|s(x_k,k)\|\left(\sigma + \frac{\|u_0\|}{\left\|B(x_k)^{-1}\right\|}\right) - \left(\sigma + \frac{\|u_0\|}{\left\|B(x_k)^{-1}\right\|}\right)^2$$

if $\left\|B(x_k)^{-1}\right\| \sigma \leq \|u_0\| \leq 2\|s(x_k,k)\| + \sigma$ holds then $\Delta V(x_k,k) \leq 0$. Hence $\|s(x_k,k)\|$ and $\left\|U_{r,k}^{eq}\right\|$, both decreases monotonically. Therefore there will be a time k_1 such that $\left\|u_{eqn}(x_k,k)\right\| \leq \|u_0\|$ for $k \geq k_1$. At that time, the control law $u_n(x_k,k)$ is applied, yielding that the solution of the system (A.5) is ultimately bounded. □

A.2 N-SML Controller

The DTSMC $v_n(x_k)$ is selected as (4.39). The convergence analysis of the N-SML control scheme is divided on neural identifier convergence and N-SML controller convergence, taking into account the discrete-time separation principle [54]. For the first analysis, it is achieved by using an EKF based algorithm to train the RHONN identifier as demonstrated in Theorem 4.1 of [36]. The tracking error convergence to a small bound region. It is achieved by the proposed controller as will be demonstrated in the following analysis Due to identification error boundedness, there exists a bounded vector valued function $\Delta_{i,k}$, which is smaller; then

$$x_k = \chi_k - \Delta_{i,k} \qquad i = 1,\ldots,r \tag{A.8}$$

with $\left\|\Delta_{i,k}\right\| \leq \gamma_i$, $\gamma_i > 0$ and r the number of the state. The sliding surface at $k+1$ is defined using x_k as follows

$$s_{n,k+1} = x_{ref,k+1} - x_{k+1} \tag{A.9}$$

Using (A.8) in (A.9), we obtain

$$s_{n,k+1} = x_{ref,k+1} - \chi_{k+1} + \Delta_{i,k} \tag{A.10}$$

with $x_{ref,k+1}$ the desired dynamics to be tracked. Using the neural linearization control part (4.39), the sliding surface is expressed as follows

$$s_{n,k+1} = x_{ref,k+1} - v_n(x_k) + \Delta_{i,k} \tag{A.11}$$

The DTSMC in (4.42) includes two cases

- When $||v_{cn}(x_k)|| \leq u_{0n}$, the control signal $v_{cn,k}$ is applied.

Using (4.43) and (4.45) in (A.10), the sliding surface at $k+1$ is

$$s_{n,k+1} = k_n s_{n,k} + \Delta_{i,k} \tag{A.12}$$

Let define the Lyapunov function candidate $V_k = s_{n,k}^T s_{n,k}$, then its difference is given as

$$
\begin{aligned}
\Delta V_k &= s_{n,k+1}^T s_{n,k+1} - s_{n,k}^T s_{n,k} \\
&= (k_n s_{n,k} + \Delta_{i,k})^T (k_n s_{n,k} + \Delta_{i,k}) - s_{n,k}^T s_{n,k} \\
&\leq (\|k_n\| \left\|s_{n,k}\right\| + \left\|\Delta_{i,k}\right\|)^2 - \left\|s_{n,k}\right\|^2 \\
&\leq (\|k_n\| \left\|s_{n,k}\right\| + \gamma_i)^2 - \left\|s_{n,k}\right\|^2 \\
&\leq \|k_n\|^2 \left\|s_{n,k}\right\|^2 + 2\|k_n\| \left\|s_{n,k}\right\| \gamma_i + \gamma_i^2 - \left\|s_{n,k}\right\|^2 \\
&\leq -(1 - \|k_n\|^2) \left\|s_{n,k}\right\|^2 + 2\|k_n\| \left\|s_{n,k}\right\| \gamma_i + \gamma_i^2 \\
&\leq -(1-\theta_1)\eta_1 \left\|s_{n,k}\right\|^2 - \theta_1\eta_1 \left\|s_{n,k}\right\|^2 \\
&\quad +2\|k_n\| \left\|s_{n,k}\right\| \gamma_i + \gamma_i^2 \\
&\leq -(1-\theta_1)\eta_1 \left\|s_{n,k}\right\|^2 + \gamma_i^2 \\
&\quad + \left(-\theta_1\eta_1 \left\|s_{n,k}\right\| + 2\|k_n\| \gamma_i\right) \left\|s_{n,k}\right\|
\end{aligned}
$$

with $0 < \theta_1 < 1$, $\eta_1 = (1 - \|k_n\|^2)$ and $\eta_1 > 0$, and for the region $\left\|s_{n,k}\right\| \geq \frac{2\gamma_i\|k_n\|}{\theta_1\eta_1}$, we obtain

$$
\begin{aligned}
\Delta V_k &\leq -(1-\theta_1)\eta_1 \left\|s_{n,k}\right\|^2 + \gamma_i^2 \\
\Delta V_k &\leq -(1-\theta_2)\beta_1 \left\|s_{n,k}\right\|^2 - \theta_2\beta \left\|s_{n,k}\right\|^2 + \Gamma^2 \\
\Delta V_k &\leq -(1-\theta_2)\beta_1 \left\|s_{n,k}\right\|^2
\end{aligned}
$$

with $0 < \theta_2 < 1$, $\beta_1 = (1-\theta_1)\eta_1$ and $\beta_1 > 0$. Therefore $\Delta V_k \leq 0$, $\forall \left\|s_{n,k}\right\| \geq \sqrt{\frac{\gamma_i^2}{\theta_2\beta_1}}$, and the solution of system (A.10) is ultimately bounded.

- When $||v_{cn}(x_k)|| > v_{0n}$, the following control law $u_0 \frac{v_{eqn}(x_k)}{\left\|v_{eqn}(x_k)\right\|}$ is applied.

Let us define the equivalent control by imposing $s_{n,k} - x_{ref,k} + \chi_k = 0$. The equivalent control is defined as

$$
\begin{aligned}
v_{eqn,k} &= s_{n,k} - x_{ref,k} + \chi_k + x_{ref,k+1} \\
&= s_{n,k} + f_{n,k}
\end{aligned} \tag{A.13}
$$

with $f_{n,k} = -x_{ref,k} + \chi_k + x_{ref,k+1}$. Then, the expression of the sliding mode surface is

$$
\begin{aligned}
s_{n,k+1} &= s_{n,k} - x_{ref,k} + x_k + x_{ref,k+1} - v_n(x_k) + \Delta_{i,k} \\
&= s_{n,k} + f_{n,k} - \left(u_o \frac{v_{eqn,k}}{\left\|v_{eqn,k}\right\|}\right) + \Delta_{i,k} \\
&= (s_{n,k} + f_{n,k}) \left(1 - u_0 \frac{1}{\left\|v_{eqn,k}\right\|}\right) + \Delta_{i,k}
\end{aligned}
$$

Using the Lyapunov function candidate $V_k = s_{n,k}^T s_{n,k}$, then

$$\begin{aligned}
\Delta V_k &= s_{n,k+1}^T s_{n,k+1} - s_{n,k}^T s_{n,k} \\
&\leq \left(\left\| s_{n,k} + f_{n,k} \right\| \left(1 - \|u_0\| \frac{1}{\left\| v_{eqn,k} \right\|} \right) + \Delta_{i,k} \right)^T \\
&\quad \left(\left\| s_{n,k} + f_{n,k} \right\| \left(1 - \|u_0\| \frac{1}{\left\| v_{eqn,k} \right\|} \right) + \Delta_{i,k} \right) \\
&\quad - \left\| s_{n,k} \right\|^2 \\
&\leq \left(\left\| s_{n,k} + f_{n,k} \right\| - \|u_0\| + \left\| \Delta_{i,k} \right\| \right)^2 - \left\| s_{n,k} \right\|^2
\end{aligned}$$

Suppose that the control law $\|u_n(x_k)\| \leq u_{0n}$ may vary within the domain [77], $\left\| f_{n,k} + \Delta_{i,k} \right\| \leq u_{0n}$, and $\sigma < u_{0n}$ with $\sigma = \left\| f_{n,k} + \Delta_{i,k} \right\|$ then

$$\begin{aligned}
\Delta V_k &\leq \left(\left\| s_{n,k} \right\| + \sigma - \|u_{0n}\| \right)^2 - \left\| s_{n,k} \right\|^2 \\
&\leq \left(\left\| s_{n,k} \right\| + \sigma - \|u_0\| + \left\| s_{n,k} \right\| \right) \\
&\quad \left(\left\| s_{n,k} \right\| + \sigma - \|u_0\| - \left\| s_{n,k} \right\| \right) \\
&\leq \left(2 \left\| s_{n,k} \right\| + \sigma - \|u_0\| \right) (\sigma - \|u_0\|) \\
&\leq - \left(2 \left\| s_{n,k} \right\| + \sigma - \|u_0\| \right) (\|u_0\| - \sigma)
\end{aligned} \tag{A.14}$$

If $\left\| f_{n,k} + \Delta_{i,k} \right\| \leq \|u_{0n}\| \leq \left(2 \left\| s_{n,k} \right\| + \left\| f_{n,k} + \Delta_{i,k} \right\| \right)$ holds, then $\Delta V_k \leq 0$ [36, 78]. Hence $\left\| s_{n,k} \right\|$ and $\left\| v_{eqn,k} \right\|$, both decreases monotonically.

Therefore there will be a time k_1 such that $\left\| v_{eqn,k} \right\| \leq \|u_0\|$ for $k \geq k_1$. At that time, the control law v_{cn} is applied, yielding that the solution of the system (A.12) is ultimately bounded. □

Appendix B
The Wind Turbine Modeling

B.1 Aerodynamic Model

Consider the horizontal axis wind system shown in Fig. B.1 on which v_1 is upstream wind speed of the turbine and v_2 is downstream wind speed. The kinetic energy of the mass air particle m that moves with a velocity is given as

$$E = \frac{1}{2}mv^2 \tag{B.1}$$

with E is the kinetic energy (J), m is the mass of the air particle (kg) and v is the speed (or the velocity) of the air particle (m/s), such that

$$m = \rho V \tag{B.2}$$

with ρ is the air density (kg/m^3) and V is the the volume (m^3). Taking into account the density of the air is constant, the relative change of the mass is calculated as follows

$$\dot{m} = \rho S\dot{x} \tag{B.3}$$

Knowing that the volume is obtained by multiplying the surface S by the length x. Only one dimension is considered because the amount of air varies along a single axis. Hence

$$\dot{m} = \rho Sv \tag{B.4}$$

By assuming that the wind speed is constant, the power of the air movement will be calculated as

$$P_w = \dot{E} = \frac{1}{2}\rho Sv^3 \tag{B.5}$$

E. N. Sánchez and L. Djilali, *Neural Control of Renewable Electrical Power Systems*, Studies in Systems, Decision and Control 278,
https://doi.org/10.1007/978-3-030-47443-0

Hence the absorbed power by the aerogenerator equals the power difference of downstream and upstream power

$$P_{aero} = P_{w1} - P_{w2} = \frac{1}{2}(\rho_1 S_1 v_1^3 - \rho_2 S_2 v_2^3) \tag{B.6}$$

Taking $\rho_1 = \rho_2$ and $\dot{m}_1 = \dot{m}_2$, we obtain

$$S_1 v_1 = S_2 v_2 \tag{B.7}$$

Substituting (B.7) in (B.6), the absorbed aerogenerator power is expressed as follow

$$P_{aero} = \frac{1}{2}\rho_1 S_1 v_1 (v_1^2 - v_2^2) \tag{B.8}$$

In other hand and according to Newton's second law

$$F = \frac{\partial}{\partial t}(mv) = \frac{\partial m}{\partial t} v + m \frac{\partial v}{\partial t} \tag{B.9}$$

Considering the wind speed is constant and the mass quantity is variable, the force relation is rewritten as

$$F = \dot{m} v \tag{B.10}$$

Substituting (B.4) in (B.10), the applied force F on the wind turbine blade is expressed as

$$F = \rho S v^2 \tag{B.11}$$

The force variation between the two sides of the aerogenerator multiplied by the wind speed result the expression of absorbed power which is expressed by the following relation

$$P_{aero} = \Delta F v = \rho S_1 v_1 (v_1 - v_2) v \tag{B.12}$$

Note that the power relationship is defined by the wind speed before and after the turbine and another wind speed named v. To define the value of the last one, we have to compare the two relationships of the wind turbine absorbed power in (B.8) and (B.12), we obtain

$$v = \frac{1}{2}(v_1 + v_2) \tag{B.13}$$

For HAWT, the air flow at wind turbine is presented in Fig. 3.4, with v_1 is the upstream wind speed, v_2 is the downstream wind speed, v is the speed of the wind passing through the aerogenerator, S_1 and S_2 are the upstream and the downstream sections of the air tube, S is the surface swept by the blade. The absorbed power by the aerogenerator in case of HAWT is calculated as follow

$$P_{aero} = \frac{1}{2}\rho S v(v_1^2 - v_2^2) \tag{B.14}$$

Using (B.13) in (B.14), we get

$$P_{aero} = \frac{1}{4}\rho S(v_1 + v_2)(v_1^2 - v_2^2) \tag{B.15}$$

and the wind power is given by

$$P_w = \frac{1}{2}\rho S v_1^3 \tag{B.16}$$

The ratio between the extracted power from the wind and the available total power available is

$$C_p = \frac{P_{aero}}{P_w} = \frac{1}{2}\left|1 - \left(\frac{v_2}{v_1}\right)^2\right|\left|1 + \left(\frac{v_2}{v_1}\right)^2\right| \tag{B.17}$$

Let define the relative speed λ as

$$\lambda = \frac{v_2}{v_1} = \frac{\Omega_t r}{v} \tag{B.18}$$

with ρ is the air density, v is the wind speed, Ω_t is the rotational speed of the turbine (low shaft), and r is the radius of a blade. So the expression of the extracted power for the wind is defined as a function of the power coefficient C_p as follows

$$P_{aero} = \frac{1}{2}C_p\rho S v^3 \tag{B.19}$$

The power coefficient C_p represents the yield aerodynamics of the WT, which depends on the turbine characteristics defined by the following empirical formula for variable speed wind turbines [57]

$$C_p(\lambda, \beta) = c_1\left(c_2\frac{1}{\Lambda} - c_3\beta^x - c_4 - c_5\right)\exp\left(\frac{-c_6}{\Lambda}\right) \tag{B.20}$$

with $c_1 = 0.5; c_2 = 116; c_3 = 0.4; c_4 = 0; c_5 = 5; c_6 = 21$ and $\frac{1}{\Lambda} = \frac{1}{\lambda + 0.08\beta} - \frac{0.035}{1+\beta^3}$ where λ is the relative speed, β is the blade angle.

B.2 DC-Link Model

In order to determine the mathematical model of the GSC, balanced grid conditions are considered. The three-phase model of the GSC is written as

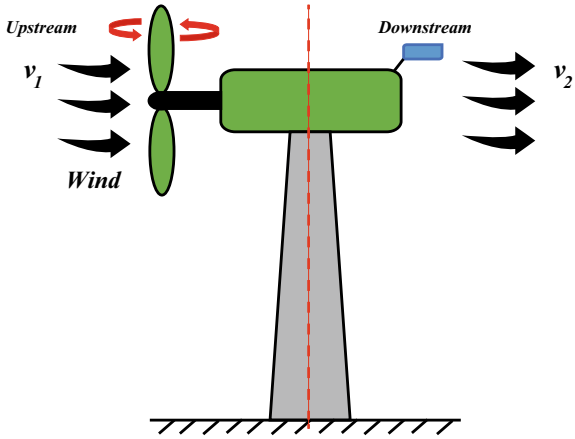

Fig. B.1 HAWT simplified scheme

$$u_{gca,t} - u_{ga,t} = -r_g i_{ga,t} + \frac{d\phi_{ga,t}}{dt} \tag{B.21}$$

$$u_{gcb,t} - u_{gb,t} = -r_g i_{gb,t} + \frac{d\phi_{gb,t}}{dt} \tag{B.22}$$

$$u_{gcc,t} - u_{gc,t} = -r_g i_{gc,t} + \frac{d\phi_{gc,t}}{dt} \tag{B.23}$$

and

$$\phi_{ga,t} = l_g i_{ga,t} \tag{B.24}$$

$$\phi_{gb,t} = l_g i_{gb,t} \tag{B.25}$$

$$\phi_{gc,t} = l_g i_{gc,t} \tag{B.26}$$

where $i_{g,t}^{abc}$ are the three-phase grid currents (A), $u_{g,t}^{abc}$ are the three phase grid voltages (V), $u_{gc,t}^{abc}$ are the three phase GSC voltages (V), which are present the control input of the DC-link voltage, r_g is the grid line resistance (Ω) and l_g is the grid inductance (H).

Substituting (B.21)–(B.23) in (B.24)–(B.26), the GSC model can be rewritten as

$$u_{gca,t} - u_{ga,t} = r_g i_{ga,t} + l_g \frac{di_{ga,t}}{dt} \tag{B.27}$$

$$u_{gcb,t} - u_{gb,t} = r_g i_{gb,t} + \frac{di_{gb,t}}{dt} \tag{B.28}$$

$$u_{gcc,t} - u_{gc,t} = r_g i_{gc,t} + \frac{di_{gc,t}}{dt} \tag{B.29}$$

$$l_g \frac{di_{g,t}^{abc}}{dt} = -r_g i_{ga,t}^{abc} - u_{g,t}^{abc} + u_{gc,t}^{abc} \tag{B.30}$$

The GSC converter can be expressed in $d-q$ by using the following transformation

$$K_g^{-1} = \frac{3}{2}\begin{bmatrix} \cos(\theta_g) & -\sin(\theta_g) & 1 \\ \cos(\theta_g - \frac{2\pi}{3}) & -\sin(\theta_g - \frac{2\pi}{3}) & 1 \\ \cos(\theta_g + \frac{2\pi}{3}) & \sin(\theta_g + \frac{2\pi}{3}) & 1 \end{bmatrix} \tag{B.31}$$

with θ_g is the grid angular position. Now, Applying the Park transformation to (B.30), we get

$$l_g \frac{d}{dt} K_g^{-1} i_{g,t}^{abc} = -r_g K_g^{-1} i_{ga,t}^{abc} - K_g^{-1} u_{g,t}^{abc} + K_g^{-1} u_{gc,t}^{abc} \tag{B.32}$$

then,

$$l_g \frac{d}{dt} i_{g,t}^{dq0} + l_g i_{g,t}^{dq0} \left((K_g) \frac{d}{dt} (K_g^{-1}) \right) = -r_g i_{ga,t}^{dq0} - u_{g,t}^{dq0} + u_{gc,t}^{dq0} \tag{B.33}$$

such that $\left((K_g)\frac{d}{dt}(K_g^{-1})\right) = W_g = \begin{bmatrix} 0 & -\omega_g s \\ 0\ \omega_g & 0 \\ 0\ 0 & 0 \end{bmatrix}$, Hence, the GSC in $d-q$ reference frame is obtained as

$$\frac{d}{dt} i_{g,t}^{dq0} = -\frac{r_g}{l_g} i_{g,t}^{dq0} - W_g i_{g,t}^{dq0} - u_{g,t}^{dq0} + u_{gc,t}^{dq0} \tag{B.34}$$

where $di_{gd,t}, di_{gq,t}$ are the $d-q$ component of the grid current, $u_{gd,t}, u_{gq,t}$ are the grid voltage $d-q$ component, and $u_{gdc,t} - u_{gqc,t}$ are the GSC voltage $d-q$ component. Neglecting the harmonics distortion due by the electronic switches, the GSC and electrical transformer losses, and the power balance between the ac and dc sides of the GSC, the DC voltage at the output of the DC link can be determined as [12]

$$\frac{dU_{dc,t}}{dt} = \frac{3}{2c_g U_{dc,t}} \left(i_{gd,t} u_{gd,t} + i_{gq,t} u_{gq,t} \right) \tag{B.35}$$

B.3 DFIG Model

The three phase stator and rotor mathematical model of the DFIG is described as

- **The DFIG Stator Equations**

$$\frac{d\phi_{s,t}^{abc}}{dt} = u_{s,t}^{abc} - r_s i_{s,t}^{abc} \tag{B.36}$$

$$\phi_{s,t}^{abc} = L_{ss} i_{s,t}^{abc} + M_{sr} i_{r,t}^{abc} \tag{B.37}$$

- **The DFIG Rotor Equations**

$$\frac{d\phi_{r,t}^{abc}}{dt} = u_{r,t}^{abc} - r_r i_{r,t}^{abc} \tag{B.38}$$

$$\phi_{r,t}^{abc} = L_{rr} i_{r,t}^{abc} + M_{rs} i_{s,t}^{abc} \tag{B.39}$$

with

$$L_{ss} = \begin{bmatrix} L_{ls} + L_{ss} & M_s & M_s \\ M_s & L_{ls} + L_{ss} & M_s \\ M_s & M_s & L_{ls} + L_{ss} \end{bmatrix}, \quad L_{rr} = \begin{bmatrix} L_{lr} + L_{rr} & M_r & M_r \\ M_r & L_{lr} + L_{rr} & M_r \\ M_r & M_r & L_{lr} + L_{rr} \end{bmatrix},$$

$$M_{sr} = M_{rs}^T = M_{sr} \begin{bmatrix} \cos(\theta) & \cos(\theta + \frac{2\pi}{3}) & \cos(\theta - \frac{2\pi}{3}) \\ \cos(\theta - \frac{2\pi}{3}) & \cos(\theta) & \cos(\theta + \frac{2\pi}{3}) \\ \cos(\theta + \frac{2\pi}{3}) & \cos(\theta - \frac{2\pi}{3}) & \cos(\theta) \end{bmatrix},$$

with $u_{s,t}^{abc}$ are the three-phase stator voltages (V), $i_{s,t}^{abc}$ are the three-phase stator currents (A), $\phi_{s,t}^{abc}$ are the three-phase stator flux (Wb), $u_{r,t}^{abc}$ are the three-phase rotor voltages (V), $i_{r,t}^{abc}$ are the three-phase rotor currents (A), $\phi_{r,t}^{abc}$ are the three-phase rotor flux (Wb), r_s is the stator winding per phase leakage resistance (Ω), r_r is the rotor winding per phase leakage resistance (Ω), L_{ls} is the stator winding per phase leakage inductance, L_{ss} is the stator self inductance, L_{lr} is the rotor winding per phase leakage inductance, L_{rr} is the rotor self inductance, M_{sr} is the stator to rotor mutual inductance, M_{rr} is the rotor to stator mutual inductance, M_s is the stator mutual inductance, and M_r is the rotor mutual inductance.

The DFIG stator variables can be expressed in $d-q$ reference frame by using the following transformation

$$K_s^{-1} = \frac{3}{2} \begin{bmatrix} \cos(\theta_s) & -\sin(\theta_s) & 1 \\ \cos(\theta_s - \frac{2\pi}{3}) & -\sin(\theta_s - \frac{2\pi}{3}) & 1 \\ \cos(\theta_s + \frac{2\pi}{3}) & \sin(\theta_s + \frac{2\pi}{3}) & 1 \end{bmatrix} \tag{B.40}$$

$$\frac{d}{dt} K_s^{-1} \phi_{s,t}^{dq0} = K_s^{-1} u_{s,t}^{dq0} - r_s K_s^{-1} i_{s,t}^{dq0} \tag{B.41}$$

$$K_s^{-1} \phi_{s,t}^{dq0} = K_s^{-1} L_{ss} i_{s,t}^{dq0} + K_s^{-1} M_{sr} i_{r,t}^{dq0} \tag{B.42}$$

then,

$$\frac{d}{dt} \phi_{s,t}^{dq0} = u_{s,t}^{dq0} - r_s i_{s,t}^{dq0} - \left(K_s \frac{d}{dt} K_s^{-1} \right) \phi_{s,t}^{dq0} \tag{B.43}$$

$$\phi_{s,t}^{dq0} = K_s L_{ss} i K_s^{-1} i_{s,t}^{dq0} + K_s M_{sr} K_s^{-1} i_{r,t}^{dq0} \tag{B.44}$$

such that $\left((K_s)\frac{d}{dt}(K_s^{-1})\right) = W_s = \begin{bmatrix} 0 & -\omega_s \\ 0\ \omega_s & 0 \\ 0\ 0 & 0 \end{bmatrix}$,

$$\frac{d}{dt}\phi_{s,t}^{dq0} = u_{s,t}^{dq0} - r_s i_{s,t}^{dq0} - W_s i \phi_{s,t}^{dq0} \tag{B.45}$$

$$\phi_{s,t}^{dq0} = l_s i_{s,t}^{dq0} + l_m i_{r,t}^{dq0} \tag{B.46}$$

with $K_s L_{ss} i K_s^{-1} = l_s$ and $K_s M_{sr} K_s^{-1} = l_m$.

The DFIG rotor variables can be expressed in $d-q$ reference frame by using the same transformation as in () by changing $(\theta_s - \theta_r)$

$$\frac{d}{dt}K_r^{-1}\phi_{r,t}^{dq0} = K_r^{-1}u_{r,t}^{dq0} - r_r K_r^{-1} i_{r,t}^{dq0} \tag{B.47}$$

$$K_r^{-1}\phi_{r,t}^{dq0} = K_r^{-1}L_{rr} i_{s,t}^{dq0} + K_r^{-1} M_{rs} i_{s,t}^{dq0} \tag{B.48}$$

then,

$$\frac{d}{dt}\phi_{r,t}^{dq0} = u_{r,t}^{dq0} - r_r i_{r,t}^{dq0} - \left(K_r \frac{d}{dt} K_r^{-1}\right)\phi_{r,t}^{dq0} \tag{B.49}$$

$$\phi_{r,t}^{dq0} = K_r L_{rr} i K_r^{-1} i_{r,t}^{dq0} + K_r M_{rs} K_r^{-1} i_{s,t}^{dq0} \tag{B.50}$$

such that $\left((K_r)\frac{d}{dt}(K_r^{-1})\right) = W_r = \begin{bmatrix} 0 & 0 & \omega_r - \omega_s \\ 0\ \omega_s - \omega_r & & 0 \\ 0 & 0 & 0 \end{bmatrix}$,

$$\frac{d}{dt}\phi_{r,t}^{dq0} = u_{r,t}^{dq0} - r_r i_{r,t}^{dq0} - W_r \phi_{r,t}^{dq0} \tag{B.51}$$

$$\phi_{r,t}^{dq0} = l_r i_{r,t}^{dq0} + l_m i_{s,t}^{dq0} \tag{B.52}$$

with $K_r L_{rr} i K_r^{-1} = l_r$ and $K_r M_{rs} K_r^{-1} = l_m$.

References

1. Sadeghkhani, I., Golshan, M.E., Mehrizi-Sani, A., Guerrero, J.M.: Low-voltage ride-through of a droop-based three-phase four-wire grid-connected microgird. IET Gener. Transm. Distrib. **12**(8), 1906–1914 (2018)
2. Yazdanian, M., Mehrizi-Sani, A.: Distributed control techniques in microgrids. IEEE Trans. Smart Grid **5**(6), 2901–2909 (2014)
3. Olivares, D., Mehrizi-Sani, A., Etemadi, A., Canizares, C., Iravani, R., Kazerani, M., Hajimiragha, A., Gomis-Bellmunt, O., Saeedifard, M., Palma-Behnke, R., Jimenez-Estevez, G., Hatziargyriou, N.: Trends in microgrid control. IEEE Trans. Smart Grid **5**(4), 1905–1919 (2014)
4. Morshed, M.J., Fekih, A.: A fault-tolerant control paradigm for microgrid-connected wind energy systems. IEEE Syst. J. **12**(1), 360–372 (2018)
5. Nasiri, M., Milimonfared, J., Fathi, S.: A review of low-voltage ride-through enhancement methods for permanent magnet synchronous generator based wind turbines. Renew. Sustain. Energy Rev. **47**, 399–415 (2015)
6. Ma, K., Chen, W., Liserre, M., Blaabjerg, F.: Power controllability of a three-phase converter with an unbalanced AC source. IEEE Trans. Power Electron. **30**(3), 1591–1604 (2015)
7. Yang, Y., Blaabjerg, F., Zou, Z.: Benchmarking of grid fault modes in single-phase grid-connected photovoltaic systems. IEEE Trans. Ind. Appl. **49**(5), 2167–2176 (2013)
8. National geographic: wind power
9. Kearney, J.: Grid voltage unbalance and the integration of DFIG. Doctoral thesis, Dublin Institute of Technology, Dublin, Ireland (2013)
10. U.S. energy information and administration: types of wind turbines
11. Tanvir, A.A., Merabet, A., Beguenane, R.: Real-time control of active and reactive power for doubly fed induction generator (DFIG)-based wind energy conversion system. Energies **8**(9), 10 389–10 408 (2015)
12. Djilali, L., Sanches, E.N., Belkheiri, M.: Real-time implementation of sliding lode field oriented control for a DFIG based wind turbine. Int. Trans. Electr. Energy Syst. **28**(9), e2539 (2018)
13. Ezzat, M., Benbouzid, M., Muyeen, S., Harnefors, L.: Low-voltage ride-through techniques for DFIG-based wind turbines: state-of-the-art review and future trends. In: 39th Annual Conference of the IEEE Industrial Electronics Society, Vienna, Austria, 10–13 Nov 2013, pp. 7681–7686 (2013)

E. N. Sánchez and L. Djilali, *Neural Control of Renewable Electrical Power Systems*, Studies in Systems, Decision and Control 278,
https://doi.org/10.1007/978-3-030-47443-0

14. Martinez, M., Tapia, G., Susperregui, A., Camblong, H.: Sliding-mode control of a wind turbine-driven double-fed induction generator under non-ideal grid voltages. IET Renew. Power Gener. **7**(4), 370–379 (2013)
15. Low voltage ride-through protection techniques for DFIG wind generator. In: 2013 IEEE Power and Energy Society General Meeting, Vancouver, BC, Canada, 21–25 July 2013
16. Yang, J., Fletcher, J.E., O'Reilly, J.A.: Series-dynamic-resistor-based converter protection scheme for doubly-fed induction generator during various fault conditions. IEEE Trans. Energy Convers. **25**, 422–432 (2010)
17. Kiani, M., Lee, W.: Effects of voltage unbalance and system harmonics on the performance of doubly fed induction wind generators. IEEE Trans. Ind. Appl. **46**(2), 562–568 (2010)
18. Sun, D., Wang, X., Nian, H., Zhu, Z.Q.: A sliding-mode direct power control strategy for DFIG under both balanced and unbalanced grid conditions using extended. IEEE Trans. Power Electron. **33**(2), 1313–1322 (2018)
19. Ornelas-Tellez, F., Rico-Melgoza, J.J., Espinosa-Juarez, E., Sanchez, E.N.: Optimal and robust control in DC microgrids. IEEE Trans, Smart Grid (2018)
20. Utkin, V.I., Guldner, J., Shi, J.: Sliding Mode Control in Electro-mechanical Systems. CRC Press, New York (2009)
21. Barambones, O.: Sliding mode control strategy for wind turbine power maximization system. Energies **5**(7), 2310–2330 (2012)
22. Beltran, B., Benbouzid, M.E., Ahmed-Ali, T.: Second-order sliding mode control of a doubly fed induction generator driven wind turbine. IEEE Trans. Energy Convers. **27**(2), 261–269 (2012)
23. Barambones, O., Cortajarena, J.A., Alkorta, P., de Durana, J.M.G.: A real-time sliding mode control for a wind energy system based on a doubly fed induction generator. Energies **7**(10), 6412–6433 (2014)
24. Patnaik, R.K., Dash, P.K., Mahapatra, K.: Adaptive terminal sliding mode power control of DFIG based wind energy conversion system for stability enhancement. Int. Trans. Electr. Energy Syst. **26**(4), 750–782 (2016)
25. Payam, A.F., Hashemnia, N., Kashiha, A.: Robust speed sensorless control of doubly-fed induction machine based on input-output feedback linearization control using a sliding-mode observer. World Appl. Sci. J. **10**(11), 1392–1400 (2010)
26. Sanchez, E., Riemann, R.: Doubly Fed Induction Generators: Control for Wind Energy. CRC Press, Taylor & Francis Group, Boca Raton (2016)
27. Xu, L., Wang, Y.: Dynamic modeling and control of DFIG-based wind turbines under unbalanced network conditions. IEEE Trans. Power Syst. **22**(1), 314–323 (2007)
28. Hu, J., He, Y.: Reinforced control and operation of DFIG-based wind-power-generation system under unbalanced grid voltage conditions. IEEE Trans. Energy Convers. **24**(4), 905–915 (2009)
29. Hu, L.X.J., He, Y., Williams, B.W.: Improved control of DFIG systems during network unbalance using PI-R current regulators. IEEE Trans. Ind. Electron. **56**(2), 439–451 (2009)
30. Soe, Y., Aung, S., Linn, Z.: Analysis on performance of DC micro-grid under fault condition. Am. Sci. Res. J. Eng. Technol. Sci. **26**(3), 1–12 (2016)
31. Lee, W.G., Nguyen, T.T., Yoo, H.J., Kim, H.M.: Low-voltage ride-through operation of grid-connected microgrid using consensus-based distributed control. Energies **11**(11), 2867 (2018)
32. Bidram, A., Lewis, F.L., Davoudi, A.: Distributed control systems for small-scale power networks: using multiagent cooperative control theory. IEEE Control Syst. Mag. **34**(6), 56–77 (2014)
33. Lopes, J.A.P., Moreira, C.L., Madureira, A.G.: Defining control strategies for microgrids in islanded operation. IEEE Trans. Power Syst. **21**(2), 916–924 (2006)
34. Hatziargyriou, N.: Microgrids Architectures and Control. Wiley, The Atrium, Southern Gate (2009)
35. Rovithakis, G.A., Chistodoulou, M.A.: Adaptive Control with Recurrent High Order Neural Networks. Springer Science & Business Media, New York (2012)
36. Sanchez, E.N., Alanis, A.Y., Loukianov, A.G.: Discrete-Time High Order Neural Control: Trained with Kalman Filtering. Springer Science & Business Media, New York (2008)

37. Ruiz-Cruz, R., Sanchez, E.N., Loukianov, A., Ruz-Hernandez, J.A.: Real-time neural inverse optimal control for a wind generator. IEEE Trans. Sustain, Energy (Early Access) (2018)
38. Zheng, X., Chen, X.: Enhancement on transient stability of LVRT of DFIG based on neural network D-STATCOM and crowbar. In: 11th IEEE International Conference on Anti-counterfeiting, Security, and Identification, Xiamen, China, 27–29 Oct 2017, pp. 64–68
39. Saidi, A.S., Helmy, W.: Artificial neural network-aided technique for low voltage ride-through wind turbines for controlling the dynamic behavior under different load conditions. Wind Eng. **43**(4), 420–440 (2019)
40. Lin, F.J., Lu, K.C., Ke, T.H., Yang, B.H., Chang, Y.R.: Reactive power control of three-phase grid-connected PV system during grid faults using Takagi-Sugeno-Kang probabilistic fuzzy neural network control. IEEE Trans. Ind. Electron. **62**(9), 5516–5528 (2015)
41. Adounia, A., Chariaga, D., Diallob, D., Hameda, M.B., Sbita, L.: FDI based on artificial neural network for low-voltage-ride-through in DFIG-based wind turbine. ISA Trans. **64**, 353–364 (2016)
42. Djilali, L., Sanchez, E.N., Belkheiri, M.: Real-time neural sliding mode field oriented control for a DFIG based wind turbine under balanced and unbalanced grid conditions. IET Renew. Power Gener. (Early Access) (2019)
43. Utkin, V.I.: Sliding mode control design principles and applications to electric drives. IEEE Trans. Ind. Electron. **40**(1), 23–36 (1993)
44. Drakunov, S., Utkin, V.: On discrete-time sliding modes. Nonlinear Control Syst. Des. IFAC Proc. **22**(3), 273–278 (1989)
45. Sanchaz, E.N., Ornelas-Tellez, F.: Discrete-Time Inverse Optimal Control for Nonlinear Systems. CRC Press, Taylor and Francis Group, Boca Raton (2013)
46. Varga, A.: A schur method for pole assigment. IEEE Trans. Autom. Control **26**(2), 517–519 (1981)
47. Freeman, R.A., Kokotovi, P.V.: Robust Nonlinear Control Design: State-Space and Lyapunov Techniques. Birkhauser, Cambridge (1996)
48. Alanis, A.Y., Sanchez, E.N., Loukianov, A.G.: Discrete-time adaptive backstepping nonlinear control via high-order neural networks. IEEE Trans. Neural Netw. **18**(4), 1185–1195 (2007)
49. Feldkamp, D.P.L., Feldkamp, T.: Conditioned adaptive behavior from Kalman filter trained recurrent networks. Proceedings of the International Joint Conference on Neural Networks **4**, 3017–3021 (2003)
50. Song, Y., Grizzle, J.W.: The extended Kalman filter as local asymptotic observer for discrete-time nonlinear systems. J. Math. Syst. Estim. Control **5**(1), 59–78 (1995)
51. Felix, R.A.: Variable structure neural control. Guadalajara Jalisco Mexico: Ph.D. dissertation, Cinvestav, Guadalajara Unit (2004)
52. Cotter, N.: The Stone Weierstrass theorem and its application to neural networks. IEEE Trans. Neural Netw. **1**(4), 290–295 (1990)
53. Krstic, M., Kanellakopoulos, I., Kokotovic, P.: Nonlinear and Adaptive Control Design. Wiley, New York (1995)
54. Lin, W., Byrnes, C.I.: Design of discrete-time nonlinear control systems via smooth feedback. IEEE Trans. Autom. Control **39**(11), 2340–2346 (1994)
55. Abad, G., Lopez, J., Rodriguez, M., Marroyo, L., Iwanski, G.: Doubly Fed Induction Machine: Modeling and Control for Wind Energy Generation. Wiley, New York (2011)
56. Jha, A.R.: Wind Turbine Technology. CRC Press, Taylor & Francis Group, Boca Raton (2011)
57. Poitiers, F., Bouaouiche, T., Machmoum, M.: Advanced control of a doubly-fed induction generator for wind energy conversion. Electr. Power Syst. Res. **79**(7), 1085–1096 (2009)
58. Betz, A.: (D.G. Randall, Introduction to the Theory of Flow Machines). Pergamon Press, Oxford (1996)
59. Oyague, F.: Gearbox modeling and load simulation of a baseline $750 - kw$ wind turbine using state-of-the art simulation codes. Technical report, National Renewable Energy Laboratory, vol. NERL/TP-500-41160, pp. 10–20 (2009)
60. Manwell, J.F., McGowan, J.G., Rogers, A.L.: Wind Energy Explained: Theory, Design and Application. Wiley, New York

61. Kearney, J.: Grid voltage unbalance and the integration of DFIG's. Doctor of philosophy, School of Electrical and Electronic Engineering the Dublin Institute of Technology (2013)
62. Recommended practices and requirements for harmonic control in electrical power systems. IEEE, Standard (1993)
63. IEEE standard for interconnecting distributed resources with electric power systems. IEEE, Standard (2014)
64. Pena, R., Clare, J., Asher, G.: A doubly fed induction generator using back-to-back PWM converters and its application to variable-speed wind-energy generation. IEEE Proc.-Electr. Power Appl. **143**(3), 231–241 (1996)
65. Hu, J., He, Y., Xu, L., Williams, B.: Four-quadrant dynamometer/power supply. Festo LabVolt Datasheet
66. Abdullaha, M., Yatim, A., Tan, C., Saidur, R.: A review of maximum power point tracking algorithms for wind energy systems. Renew. Sustain. Energy Rev. **16**(5), 3220–3227 (2012)
67. Bergen, A., Vital, V.: Power System Analysis. Tom Robbins, Upper Saddle River (2000)
68. Illinois center for a smarter electric grid, IEEE 09 bus system. http://publish.illinois.edu/smartergrid/
69. Pettikkattil, J.: IEEE 9 bus transmission system. https://la.mathworks.com/matlabcentral/fileexchange/45936-ieee-9-bus
70. Attou, A., Massoum, A., Saidi, M.: Photovoltaic power control using MPPT and boost converter. Balk. J. Electr. Comput. Eng. **2**(1), 23–27 (2014)
71. Kim, S.K., Lee, K.B.: Robust feedback-linearizing output voltage regulator for DC/DC boost converter. IEEE Trans. Ind. Electron. **62**(11), 7127–7135 (2015)
72. Loza-Lopez, M., Lopez-Garcia, T., Ruiz-Cruz, R., Sanchez, E.: Neural control for a micro-grid. In: International Joint Conference on Neural Network, pp. 880–887 (2017)
73. Zenginis, I., Vardakas, J.S., Abadal, J., Vardakas, C., Guell, M.M., Verikoukis, C.: Optimal power equipment sizing and management for cooperative buildings in microgrids. IEEE Trans. Ind. Inform. **15**(1), 158–172 (2019)
74. Atia, R., Yamada, N.: Sizing and analysis of renewable energy and battery systems in residential microgrids. IEEE Trans. Smart Grid **7**(1), 1204–1213 (2016)
75. Kaur, R., Kumar, D.: Transient stability improvement of IEEE 9 bus system using power world simulator. Int. J. Eng. Res. Appl. **6**, 35–39 (2016)
76. Cardenas, R., Diaz, M., Rojas, F., Clare, J., Wheeler, P.: Resonant control system for low voltage ride-through in wind energy conversion systems. IET Power Electron. **9**(6), 1297–1305 (2016)
77. Bartolini, G., Ferrara, A., Utkin, V.I.: Adaptive sliding mode control discrete-time system. Automatica **31**(5), 769–773 (1995)
78. Castaneda, C.E., Loukianov, A.G., Sanchez, E.N., Castillo-Toledo, B.: Discrete-time neural sliding-mode block control for a DC motor with controlled flux. IEEE Trans. Ind. Electron. **59**(2), 1194–1207 (2012)